

Bulleyaconitine A attenuates hyperexcitability of dorsal root ganglion neurons induced by spared nerve injury: The role of preferably blocking Nav1.7 and Nav1.3 channels

Molecular Pain
Volume 14: 1–13
© The Author(s) 2018
Reprints and permissions:
sagepub.com/journalsPermissions.nav
DOI: 10.1177/1744806918778491
journals.sagepub.com/home/mpx


Man-Xiu Xie¹, Jie Yang², Rui-Ping Pang^{2,3}, Wei-An Zeng¹,
Han-Dong Ouyang¹, Yan-Qing Liu⁴, and Xian-Guo Liu^{2,3}

Abstract

Background: Oral administration of Bulleyaconitine A, an extracted diterpenoid alkaloid from *Aconitum bulleyanum* plants, is effective for treating chronic pain in rats and in human patients, but the underlying mechanisms are poorly understood. **Results:** As the hyperexcitability of dorsal root ganglion neurons resulting from the upregulation of voltage-gated sodium (Nav) channels has been proved critical for development of chronic pain, we tested the effects of Bulleyaconitine A on Nav channels in rat spared nerve injury model of neuropathic pain. We found that Bulleyaconitine A at 5 nM increased the threshold of action potentials and reduced the firing rate of dorsal root ganglion neurons in spared nerve injury rats but not in sham rats. Bulleyaconitine A preferably blocked tetrodotoxin-sensitive Nav channels over tetrodotoxin-resistant ones in dorsal root ganglion neurons of spared nerve injury rats. Bulleyaconitine A was more potent for blocking Nav1.3 and Nav1.7 than Nav1.8 in cell lines. The half maximal inhibitory concentration (IC₅₀) values for resting Nav1.3, Nav1.7, and Nav1.8 were 995.6 ± 139.1 nM, 125.7 ± 18.6 nM, and 151.2 ± 15.4 μM, respectively, which were much higher than those for inactivated Nav1.3 (20.3 ± 3.4 pM), Nav1.7 (132.9 ± 25.5 pM), and Nav1.8 (18.0 ± 2.5 μM). The most profound use-dependent blocking effect of Bulleyaconitine A was observed on Nav1.7, less on Nav1.3, and least on Nav1.8 at IC₅₀ concentrations. Bulleyaconitine A facilitated the inactivation of Nav channels in each subtype. **Conclusions:** Preferably blocking tetrodotoxin-sensitive Nav1.7 and Nav1.3 in dorsal root ganglion neurons may contribute to Bulleyaconitine A's antineuropathic pain effect.

Keywords

Bulleyaconitine A, neuropathic pain, dorsal root ganglion, voltage-gated sodium channel, peripheral nerve injury

Date Received: 27 January 2018; revised: 16 April 2018; accepted: 24 April 2018

Background

Neuropathic pain induced by peripheral nerve injury, manifested as allodynia, hyperalgesia, and spontaneous pain, reduces patient's life quality and working ability seriously. At present, drugs for treating the disease are less effective and have various side effects (see literature^{1,2} for reviews).

Compelling evidence shows that the increased excitability of dorsal root ganglion (DRG) neurons, manifested as spontaneous activity,³ the decreased threshold, and the increased firing rate of action

¹Department of Anesthesiology, Sun Yat-Sen University Cancer Center, State Key Laboratory of Oncology in South China, Collaborative Innovation Center for Cancer Medicine, Guangzhou, China

²Department of Physiology, Pain Research Center, Zhongshan School of Medicine of Sun Yat-Sen University, Guangzhou, China

³Guangdong Provincial Key Laboratory of Brain Function and Disease, Guangdong, China

⁴Department of Pain Medicine, Beijing Tian Tan Hospital, Capital Medical University, Beijing, China

The first two authors contributed equally to this work.

Corresponding Author:

Xian-Guo Liu, Hemu Building 806, No. 74 Zhongshan Road 2, Guangzhou 510080, China.

Email: liuxg@mail.sysu.edu.cn



potentials,^{4–7} plays an important role in the development of neuropathic pain. The hyperexcitability of DRG neurons is caused by altered expression, trafficking, and functioning of many ion channels, including voltage-gated calcium channels,⁸ hyperpolarization-activated cyclic nucleotide-gated ion channels,⁹ and voltage-gated sodium (Nav) channels (see literature¹⁰ for a review).

The Nav channels, which are critical for producing and propagating action potentials, are classified into nine subtypes (Nav1.1–1.9). Among them, upregulation of tetrodotoxin-sensitive (TTX-S) Nav1.3,¹¹ Nav1.7,¹² or tetrodotoxin-resistant (TTX-R) Nav1.8¹³ is proved important for the expression of neuropathic pain. Gain of function of Nav1.7 and Nav1.8 is critical for neuropathic pain in human.¹⁴ Therefore, the channel subtypes are promising targets for treatment of neuropathic pain.

Bulleyaconitine A (BLA), a diterpenoid alkaloid extracted from *Aconitum bulleyanum* plants, has been used for treatment of chronic pain in human patients in China since 1985. Clinical data have shown that oral administration of BLA effectively relieves arthralgia and neck shoulder lumbocurral pain with minor side effect.^{15,16} BLA has a powerful analgesic effect in naive rodents.^{17,18} Oral administration of BLA alleviates neuropathic pain and long-term potentiation at C-fiber synapses in spinal dorsal horn induced by paclitaxel in rats.¹⁹ Recently, we show that BLA preferably blocks TTX-S sodium channels in DRG neurons in L5 spinal nerve ligation rats.²⁰ Previous works show that BLA at 10 μ M use-dependently block Nav1.3, Nav1.7, and Nav1.8 in GH₃ and human embryonic kidney (HEK) 293t cell lines.^{21,22} Nevertheless, the data cannot explain the analgesic effect of oral administration of BLA, as recent studies on rats show that mean peak serum concentration (C_{max}) of BLA is only 17.8 nM following oral BLA²³ at 0.4 mg/kg that is effective for inhibition of neuropathic pain.¹⁹ Recently, we show that BLA preferably inhibits the TTX-S sodium channels over TTX-R ones in lumbar 5 spinal nerve ligation model of neuropathic pain.²⁰ In the present work, we address this issue in spared nerve injury (SNI) rats, and the effects of BLA on Nav1.3, Nav1.7, and Nav1.8 were investigated in HEK 293 and ND7/23 cell lines.

Materials and methods

Subjects

Male Sprague-Dawley rats (80–200 g) were housed in separate cages at a temperature-controlled ($24 \pm 1^\circ\text{C}$) and humidity-controlled (50–60%) room with a 12:12-h light–dark cycle. They had access to food and water ad libitum. All animal experimental procedures were approved by the Animal Care and Use Committee of

Sun Yat-Sen University and were carried out in accordance with the guideline of the National Institutes of Health on the animal care and the ethical guidelines for investigation of experimental pain in conscious animal.²⁴

Surgical procedures and administration of drug

SNI was performed following the procedures described by Decosterd and Woolf.²⁵ Briefly, an incision through skin on the lateral surface of the thigh was made under anesthesia with 10% chloral hydrate (0.4 g/kg, i.p.), and the left sciatic nerve and its three terminal branches were exposed. The common peroneal and the tibial nerves were tightly ligated with a 6-0 silk and transected distal to the ligation, removing a 3 to 5 mm nerve portion. The sural nerve was remained intact, and any contact or stretch to this nerve is carefully avoided. Special care was paid to prevent infection and to minimize the influence of inflammation. The chronic indwelling peri-DRG catheter system was modified according to previous study.²⁶ The catheters were constructed from sterile gel-foam aseptically cut into 20-mm (L) \times 7-mm (W) \times 6-mm (H) strips. One end was bisected (3.5 mm W) to a depth of 1 cm to allow a 5-cm sterile polyethylene (PE-10) tube to be sutured inside. The assembly was implanted around the L4-6 DRGs. Vehicle or BLA at different concentrations (0.1, 1.0, and 10 nM in 15 μ l volume) were injected slowly (2 min) through the PE-10 tube.²⁷

DRG neurons preparation

DRG neurons were dissociated seven days after sham or SNI surgery using enzyme digestion as previously described with slight modifications.²⁸ In brief, L4-6 DRGs from ipsilateral or contralateral side of SNI operation were freed from their connective tissue sheaths and cut into pieces with a pair of sclerotic scissors in Dulbecco modified Eagle medium/F12 medium (GIBCO, United States) under low temperature (in a mixture of ice and water). After enzymatic and mechanical dissociation, DRG neurons were plated on glass coverslips coated with Poly-L-Lysine (Sigma, United States) in a humidified atmosphere (5% CO₂, 37°C) and used for electrophysiological recordings investigation approximately 4 h after plating.

Cultures of HEK 293 cells stably expressing Nav1.3 and Nav1.7

HEK 293 cells stably expressing human homolog of human Nav1.3 (SCN3A, NM_006922.3) and human Nav1.7 (SCN9A, NM_002977.3) were maintained under standard cell culture condition (5% CO₂; 37°C) in Dulbecco modified Eagle medium (Invitrogen,

Carlsbad, CA) and F-12 medium (Invitrogen) mixture at 1:1 supplemented with 10% fetal bovine serum (HyClone, Logan, UT) under selection of antibiotic G418 (Genecitin; Invitrogen) with a concentration of 500 $\mu\text{g}/\text{ml}$. Cells were passaged every three days with 0.25% Trypsin-EDTA (Invitrogen). Cells used for electrophysiology were seeded on a glass coverslip.²⁹

Transient transfection of ND7/23 cell with Nav1.8

Human Nav1.8-cDNA was subcloned into the mammalian expression vector pCMV-Script (Stratagene, La Jolla, CA), and the sequence of the entire Nav1.8 channel protein (NCBI nucleotide access number U53833) was verified by dideoxynucleotide sequencing. The ND7/23 neuroblastoma fusion cell line was purchased from Sigma (Sigma-Aldrich, St. Louis, MO) and cultured in Dulbecco's modified Eagle's medium (Invitrogen, Carlsbad, CA) supplemented with 10% fetal bovine serum (Invitrogen), 2 mM L-glutamine, 100 U/ml penicillin, and 100 $\mu\text{g}/\text{ml}$ streptomycin (Invitrogen) at 37°C under 5% CO₂. Cells were grown on 12-mm glass coverslips and transiently transfected with hNav1.8-pCMV-Script (1–3 μg) and the pEGFP-N1 (Clontech, Mountain View, CA) reporter plasmid (0.5–1 μg) using Lipofectamine LTX (Invitrogen). Patch clamp study was performed at 48 to 72 h after transfection, cells with green fluorescent were selected under fluorescence microscopy.

Whole cell patch clamp recordings

Whole-cell patch clamp recordings were performed using an EPC-10 amplifier and the PULSE program (HEKA Electronics, Lambrecht, Germany) as previously described.⁵ Currents were recorded with glass pipettes (1–3 M Ω resistance) fabricated from borosilicate glass capillaries using a Sutter P-97 puller (Sutter Instruments, Novato, CA). Membrane currents were filtered at 10 kHz and sampled at 50 kHz. Voltage errors were minimized by using 80% to 90% series resistance compensation. TTX-S and TTX-R Na⁺ currents were recorded in large (>30 μm in diameter) and small (<20 μm) DRG neurons, respectively. The effects of BLA on action potentials were tested in small and medium DRG neurons (20–35 μm in diameter). The neurons with leak current >500 pA or series resistance >10 M Ohm were discarded. For current clamp experiments on DRG neurons, the bath solution contained (in mM): 140 NaCl, 5 KCl, 2 CaCl₂, 2 MgCl₂, 10 D-glucose, 10 HEPES, pH adjusted to 7.4 with NaOH. The pipette solution contained (in mM): 30 KCl, 100 K-aspartate, 5 MgCl₂, 2 Mg-ATP, 0.1 Na₂GTP, 40 HEPES, pH adjusted to 7.2 with KOH. For voltage clamp experiments on DRG neurons, the extracellular solution contained (in mM):

30 NaCl, 20 TEA-Cl, 90 choline-Cl, 3 KCl, 1 CaCl₂, 1 MgCl₂, 10 HEPES, 10 glucose, and 0.1 CdCl₂ (adjusted to pH 7.3 with Tris base). The pipette solution contained (in mM): 135 CsF, 10 NaCl, 10 HEPES, 5 EGTA, and 2 Na₂ATP (adjusted to pH 7.2 with CsOH). Experiments on HEK 293 cells and ND7/23 cells were performed with an external solution containing (in mM): 140 NaCl, 4 KCl, 1 MgCl₂, 2 CaCl₂, 5 D-Glucose monohydrate, 10 HEPES, (adjusted to pH 7.4 with NaOH) and a pipette solution containing (in mM): 145 CsCl, 0.1 CaCl₂, 2 MgCl₂, 10 NaCl, 0.5 Na₂GTP, 2 MgATP, 1.1 EGTA, 10 HEPES (adjusted to pH 7.2 with CsOH). For recording Nav1.8 in ND7/23 cells, 300 nM TTX was included to block the TTX-S Na⁺ currents. The osmolality of all solutions was adjusted to 310 mOsm.

Pulse protocols and current measures

The action potentials of DRG neurons were recorded in current clamp mode. Action potentials were elicited by a series of depolarizing currents from 0 to 700 pA (150 ms) in 50 pA step increments. To test the effects of BLA on firing rates, the mean number of action potentials elicited by a depolarizing current (1 s duration) at double-strength of rheobase (2 \times rheobase) were measured before and 15 min after BLA (5 nM) application (Figure 2). The Na⁺ current evoked from a holding potential of –80 mV to the test pulses ranging from –90 mV to +30 mV (Figure 3(a) and (b)). After established the whole cell recording, membrane potential was hold at –90 mV, then Na⁺ current was elicited at –10 mV depolarization potential from HEK 293 and ND7/23 cells (Figure 4). To study the effect of BLA on resting Nav channels, the Na⁺ currents were recorded every 5 min after BLA application. The inactivated state of Nav channels was achieved by using a 1 s prepulse to 0 mV to inactivate the Na⁺ currents followed by a 10 ms (60 ms for Nav1.8) to –90 mV and a subsequent test impulse to –10 mV for 50 ms. An interpulse interval of 10 s allows recovery from inactivation (Figure 6). Nav1.8 currents in DRG neurons were elicited with a 500 ms step to –50 mV to inactivate the Nav1.9 current followed by a test pulses in the presence of 300 nM TTX in the bath solution (Figure 7). To test the use-dependent blockage of BLA on Nav channels, holding potential was –80 mV to the test pulse of –10 mV at different frequencies (1, 3, and 10 Hz). The amplitude of currents evoked by the *n*th impulse was normalized to the current evoked by the first impulse (Figure 8). The voltage dependence of Nav channels activation was evoked from a holding potential of –90 mV and then depolarized from –120 mV to +100 mV at 5-mV steps. Steady-state inactivation was recorded by a depolarized pulse from –120 mV to +40 mV with 5 mV increments, followed immediately by a test pulse to 0 mV.

Time constants for recovery from inactivation of Nav channels were measured with a double-pulse protocol. A first pulse (P1) for 250 ms to -10 mV caused inactivation, and Na^+ current evoked by the test pulse (P2) to -10 mV after variable intervals was compared with $I_{\text{Na}, p1}$ of the same episode.

To obtain IC_{50} values, the fractional blocks obtained at different drug concentrations were fitted with the Hill equation: $E = E_{\text{max}}/[1 + (\text{IC}_{50}/C)^b]$, where E is the inhibition of currents in percentage at concentration C , E_{max} is the maximum inhibition, IC_{50} is the concentration for 50% inhibition of maximum effect, and b is the Hill coefficient. The activation or inactivation conductance variables of I_{Na} were determined with normalized currents. Current activation and inactivation were fitted by the Boltzmann distribution: $y = 1/\{1 + \exp [(V_m - V_{0.5})/S]\}$, where V_m is the membrane potential, $V_{0.5}$ is the activation or inactivation voltage mid-point, and S is the slope factor. The relation of $1/\tau_{\text{block}}$ against the concentration is described by the linear function: $1/\tau_{\text{block}} = k[D] + l$, where $1/\tau_{\text{block}}$ is the time constant of development of block, and k and l are the apparent rate constants for association and dissociation of the drug.

Chemicals

BLA powder (Yunnan Haopy, China) were dissolved as a stock solution of 0.5 mM or 10 mM in sterilizing double-distilled water and diluted with extracellular solution or sterile saline solution to different working concentrations. BLA solution was adjusted to pH 7.35 to 7.40. Tetrodotoxin was purchased from YUANYE (Shanghai, China) and was dissolved in acetic acid aqueous solution as a stock of 1 mM, diluted to a working concentration of 300 nM for recordings on TTX-R Na^+ current or Nav1.8 current. A-803467 (Alomone Labs) was dissolved as a stock of 10 mM in DMSO and diluted to 1 μM with extracellular solution.

Statistical analysis

All data were expressed as mean \pm SD. Mathematical curve fitting and statistical analyses were performed using Prism 5 (GraphPad Software Inc., San Diego, CA) and SPSS 13.0 (SPSS, Chicago, IL). For patch clamp analysis, one-way and two-way analysis of variance (ANOVA) followed by Tukey post hoc test for multiple groups and paired Student t test was used for comparison between two groups. Behavioral data were analyzed by two-way ANOVA with repeated measures followed by Tukey post hoc test for all groups and between groups and one-way ANOVA followed by Tukey post hoc test for different groups on the same time point were carried out. The criterion for statistical significance was considered at $p < 0.05$.

Results

BLA inhibits hyperexcitability of DRG neurons induced by SNI

Our recent work shows that BLA preferably blocks Nav channels in DRG neurons of neuropathic rats over sham rats and that local application of BLA (1 or 10 nM) onto DRG ipsilateral to surgery inhibits neuropathic pain induced by L5-SNL.²⁰ To investigate whether BLA may also preferably affect the excitability of DRG neurons in SNI rats, we tested the effects of BLA at 5 nM in DRG neurons from SNI sham rats, in which paw withdrawal thresholds and paw withdrawal latencies decreased significantly. Action potentials in 48 DRG neurons with diameters ranging from 20 to 35 μm ($27.4 \pm 2.9 \mu\text{m}$) were recorded in this work, as C-fibers and A δ -fibers that conduct pain signals are axons of small and medium DRG neurons. To determine the thresholds of action potentials, a series of depolarizing currents from 0 to 700 pA (150 ms) in 50 pA step increments was delivered under current clamp mode, and a minimal current that evoked an action potential was defined as threshold (rheobase) (Figure 1(A)). We found that the threshold was significantly lower in SNI rats compared to sham rats (312.5 ± 20.6 pA vs. 470.0 ± 30.8 pA, Figure 1(A) and (C, a)). Fifteen minutes after perfusion of BLA at 5 nM, the thresholds of action potentials in SNI rats increased significantly (433.3 ± 20.1 pA), while in sham rats the thresholds did not change (488.9 ± 40.2 pA, Figure 1(A) and (C, a)). BLA enhanced the half-widths of action potentials (Figure 1(C, b)) but reduced the peak amplitude (Figure 1(C, c)) and overshoot (Figure 1(C, d)) in both sham and SNI groups. BLA reduced the rise time of action potentials in SNI group but not in sham group (Figure 1(C, e)) and did not affect input resistance in both groups (Figure 1(C, f)). To test the effects of BLA on firing rates of DRG neurons, the number of action potentials elicited by a depolarizing current (1s duration) at double-strength of rheobase ($2 \times$ rheobase) were measured before and 15 min after BLA (5 nM) application. As shown in Figure 1(B) and (D), the number of action potentials elicited by the same stimulus was significantly larger in SNI group than that in sham group. BLA reduced the number of action potentials in DRG neurons of SNI rats significantly (from 11.9 ± 1.1 to 3.5 ± 0.5) but not in sham rats (from 5.2 ± 0.9 to 3.6 ± 0.6). The inhibitory effect of BLA on the excitability of DRG neurons may contribute to its relief of neuropathic pain.

The effects of BLA on Nav channels in DRG neurons

As Nav channels are critical for generation of action potentials, we next tested the effects of BLA on TTX-S and TTX-R Na^+ currents in DRG neurons from

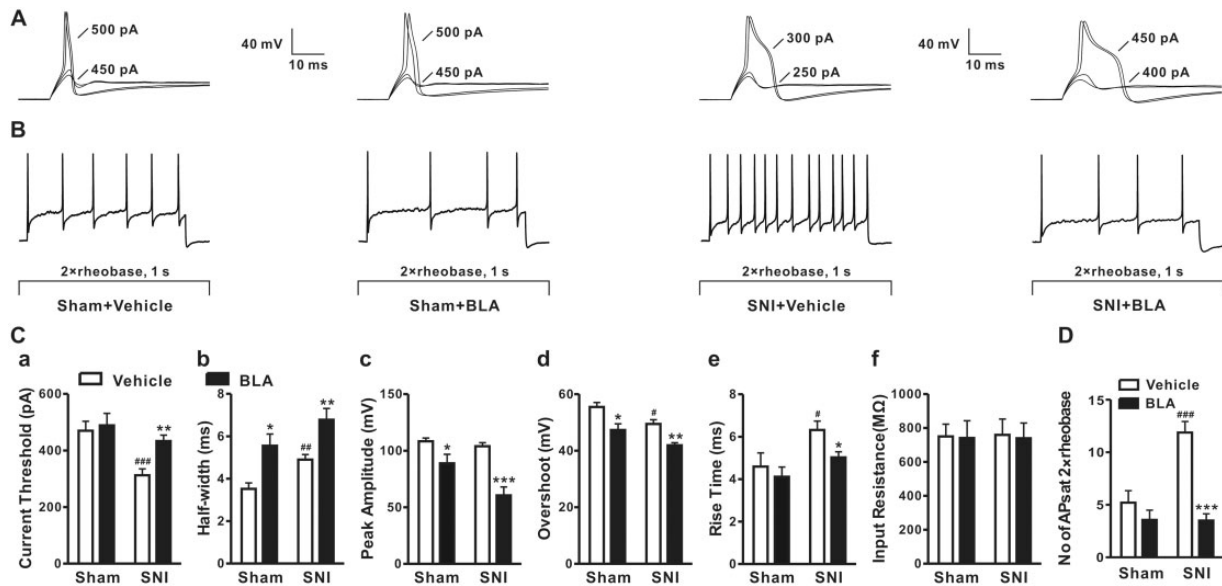


Figure 1. BLA reduces the excitability of DRG neurons from SNI rats. (A) The representative traces show the thresholds of action potentials evoked by current injections to DRG neurons from sham rats and SNI rats before and 15 min after application of BLA at 5 nM. (B) The typical traces show the action potentials elicited by 2×rheobase for 1 s in DRG neurons of sham rats and SNI rats before and after BLA. (C) The summary data show that the statistic comparison of the threshold of action potentials, half-width, the peak amplitude, the overshoot, the rise time, and the input resistance before and after BLA ($n=12$ in each group). (D) The summary data show that the statistic comparison of the numbers of action potentials in sham and SNI rats with or without BLA ($n=12$ in each group). * $p < 0.05$, ** $p < 0.01$, *** $p < 0.001$ compared to vehicle. # $p < 0.05$, ### $p < 0.01$, #### $p < 0.001$ compared to sham rats. BLA: Bulleyaconitine A; SNI: spared nerve injury.

ipsilateral or contralateral side of SNI injury. As previous works show that small-diameter DRG neurons ($<25 \mu\text{m}$) express both TTX-S and TTX-R channels, while large DRG neurons predominately express TTX-S channels,³⁰ we recorded TTX-S and TTX-R Na^+ currents in the large-diameter neurons ($>30 \mu\text{m}$) and small-diameter neurons ($<20 \mu\text{m}$), respectively. To isolated TTX-S Na^+ currents, recordings were performed in the presence of $1 \mu\text{M}$ A-803467 that blocks TTX-R Nav channels.^{31,32} The TTX-S Na^+ current were initially recognized by their relatively faster activation and inactivation. The identification was confirmed by adding 300 nM TTX at the end of the recordings. Only the current recordings that can be reduced $\geq 90\%$ with 300 nM TTX were used for further analysis (Figure 2(a) and (b)). To record TTX-R Na^+ currents, the small-diameter neurons ($<20 \mu\text{m}$) were selected, and TTX (300 nM) was included to the bath solution.³³ In DRG neurons from ipsilateral side of injury, IC_{50} for resting TTX-S Nav channels was 25 times lower than that for TTX-R Nav channels ($3.8 \pm 0.4 \text{ nM}$ vs. $94.6 \pm 11.5 \text{ nM}$, Figure 2(c)). IC_{50} for inactivated TTX-S and TTX-R Na^+ currents was only $0.5 \pm 0.1 \text{ nM}$ and $8.0 \pm 1.0 \text{ nM}$, respectively (Figure 2 (e)), which were at least eight times lower than those for resting channels. In DRG neurons from contralateral side of injury, IC_{50} values for resting TTX-S and TTX-R Na^+ currents were $64.6 \pm 7.2 \text{ nM}$ and $2.0 \pm 0.3 \mu\text{M}$,

respectively (Figure 2(d)), which are at least 17 times higher than those from ipsilateral side. And the IC_{50} values for inactivated TTX-S ($6.8 \pm 0.9 \text{ nM}$) and TTX-R ($77.3 \pm 10.5 \text{ nM}$) Na^+ currents were also much higher than those in neurons from ipsilateral side of injury (Figure 2(f)). The data indicate that BLA preferably block inactivated channels over resting channels, was more potent for blocking TTX-S Nav channels than TTX-R ones.

BLA blocks resting and inactivated Nav1.3, Nav1.7, and Nav1.8 subtypes expressed in cell lines with different potencies

Compelling evidence has demonstrated that TTX-S Nav1.3, Nav1.7, and TTX-R Nav1.8 are critically involved in neuropathic pain.^{34–36} It has been reported that BLA at a higher concentration ($10 \mu\text{M}$) does not affect resting and inactivated Nav1.3, Nav1.7, and Nav1.8 in cell lines, when measured 5 min after external application.^{21,22} In line with the finding, we found that BLA blocked resting Nav1.3, Nav1.7, and Nav1.8 currents 15 min but not 5 min after application (Figure 3(a), bottom panel). While in vehicle-treated cells, little change of Na^+ currents in all the subtypes within 15 min was observed (Figure 3(a), top panel).

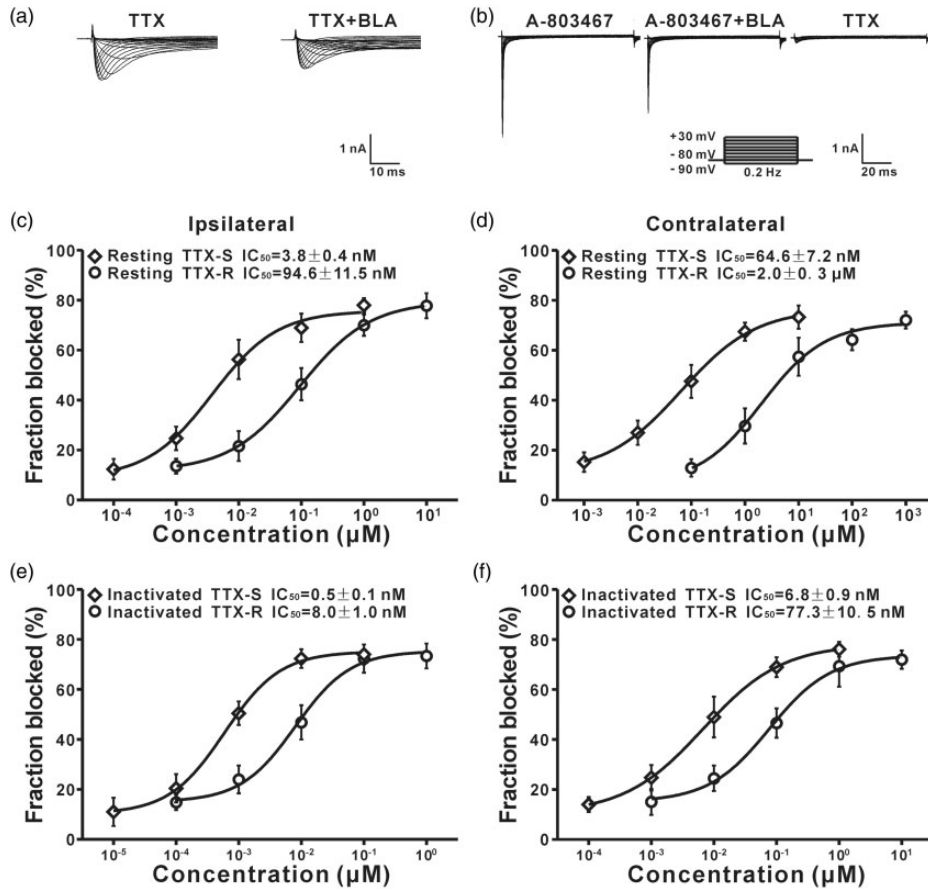


Figure 2. The differential effects of BLA on TTX-S and TTX-R Nav channels in DRG neurons from ipsilateral and contralateral side of SNI injury. (a) Representative traces show TTX-R Na⁺ currents recorded in the presence of 300 nM TTX with or without 10 nM BLA. (b) TTX-S currents were recorded in the presence of 1 μM A-803467, 1 μM A-803467, and 1 nM BLA or 300 nM TTX. (c) IC₅₀ values of BLA on resting TTX-S ($n = 8$ in each data point) and TTX-R ($n = 7$ at each data point) Nav channels in DRG neurons from ipsilateral side of injury. (d) IC₅₀ values of BLA on resting TTX-S ($n = 6$ at each data point) and TTX-R ($n = 8$ at each data point) Nav channels in DRG neurons from contralateral side of injury. (e) IC₅₀ values of BLA on inactivated TTX-S and TTX-R Nav channels in DRG neurons from ipsilateral side of injury ($n = 7$ at each data point). (f) IC₅₀ values of BLA on inactivated TTX-S and TTX-R Nav channels in DRG neurons from contralateral side of injury ($n = 8$ each data point).

BLA: Bulleyaconitine A; TTX-R: tetrodotoxin-resistant; TTX-S: tetrodotoxin-sensitive.

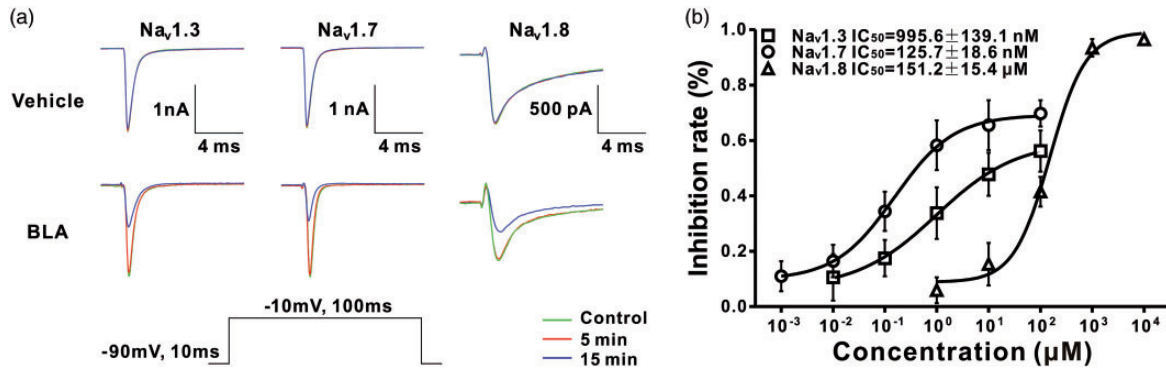


Figure 3. BLA blocks resting Nav1.3, Nav1.7, and Nav1.8 subtypes with different potency. (a) The current traces were recorded before (control) and 5 min, 15 min after vehicle (top traces), or BLA application at IC₅₀ concentrations (bottom traces). The Na⁺ currents were elicited by a voltage protocol shown in the inset. (b) IC₅₀ values for Nav1.3, Nav1.7, and Nav1.8 ($n = 10$ cells in each data points).

BLA: Bulleyaconitine A.

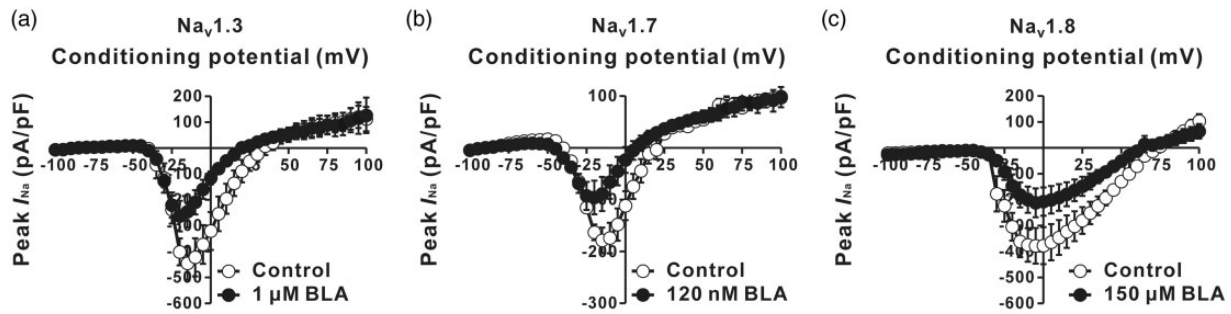


Figure 4. The effects of BLA on current–voltage curves of Nav1.3, Nav1.7, and Nav1.8 currents. (a) to (c) The currents were recorded before (control) and 15 min after BLA applications at corresponding IC₅₀ concentrations of the channel subtypes ($n=9$ cells in each data point).

BLA: Bulleyaconitine A.

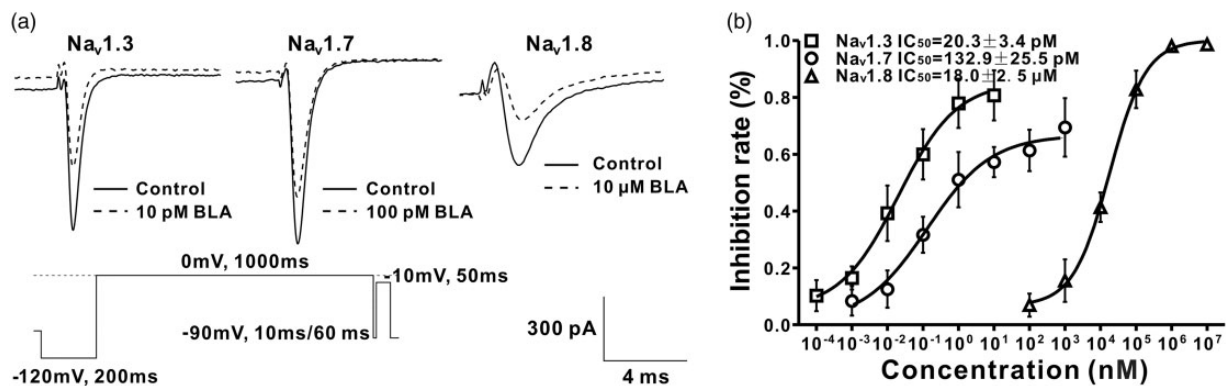


Figure 5. BLA differentially blocks inactivated Nav1.3, Nav1.7, and Nav1.8. (a) The representative current traces recorded before (control) and 15 min after BLA application at indicated concentrations and the protocol for inactivation of Nav channels. (b) IC₅₀ values of BLA on the channel subtypes are shown ($n=8$ cells in each data point).

BLA: Bulleyaconitine A.

Table 1. The IC₅₀ values in different Nav channel subtypes.

	Nav1.8	Nav1.7	Nav1.3
Resting state	151.2 ± 15.4 μM	125.7 ± 18.6 nM (1203)	995.6 ± 139.1 nM (152)
Inactivated state	18.0 ± 2.5 μM	132.9 ± 25.5 pM (135,440)	20.3 ± 3.4 pM (886,670)
Times	8	946	49,044

Note: The times indicate fold differences in IC₅₀ between resting and inactivated states. The digits in round brackets indicate fold differences in IC₅₀, compared to Nav1.8.

At resting state, IC₅₀ for Nav1.3 and Nav1.7 was, respectively, 995.6 ± 139.1 nM and 125.7 ± 18.6 nM, which was much lower than that for Nav1.8 (151.2 ± 15.4 μM) (Figure 3(b)). Consistently, the I to V curves revealed that the peak amplitudes of Na⁺ currents were reduced to ~50% by BLA at the IC₅₀ concentrations in each channel subtype (Figure 4(a) to (c)). While IC₅₀ values for inactivated Nav1.3, Nav1.7, and Nav1.8 were only 20.3 ± 3.4 pM, 132.9 ± 25.5 pM, and 18.0 ± 2.5 μM, respectively (Figure 5(b)), which were

much lower compared with those at resting states (Table 1). Figure 5(a) showed the typical current traces recorded before and after BLA application at indicated concentrations. The data demonstrated that BLA preferably blocked Nav1.3 and Nav1.7 expressed in HEK 293 cell line over Nav1.8 in ND7/23 cell line and is more potent for blocking inactivated Nav channels than resting ones.

To determine whether the different effects of BLA may be due to the difference in cell line, we tested the

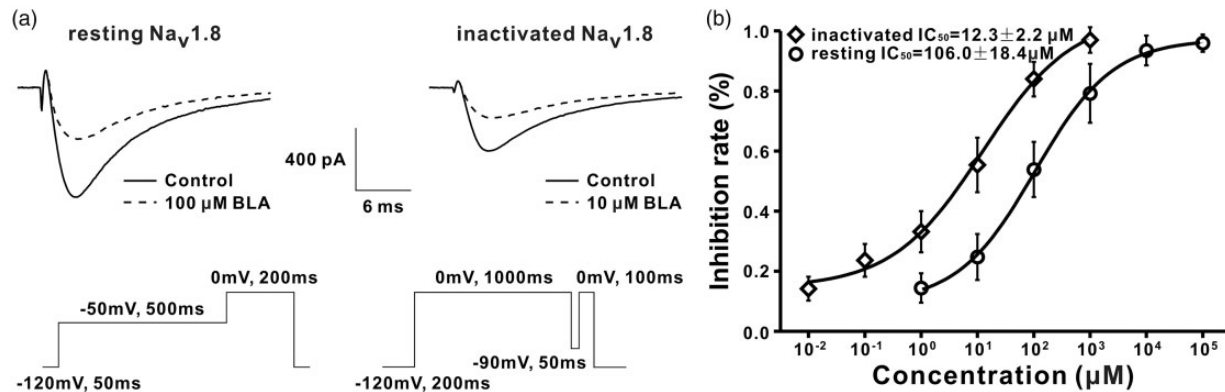


Figure 6. BLA blocks resting and inactivated Nav1.8 in DRG neurons with different potency. IC₅₀ values for the resting and inactivated Nav1.8 are shown ($n = 7$ neurons in each data point). BLA: Buleyaconitine A.

effect of BLA on isolated Nav1.8 currents in DRG neurons and found that IC₅₀ for resting and inactivated Nav1.8 was $106.0 \pm 18.4 \mu\text{M}$ and $12.3 \pm 2.2 \mu\text{M}$, respectively (Figure 6), which are comparable to those in ND7/23 cells ($151.2 \pm 15.4 \mu\text{M}$ and $18.0 \pm 2.5 \mu\text{M}$; Figures 3 and 5).

The use-dependent blockage of BLA is most potent on Nav1.7, less on Nav1.3, and least on Nav1.8

Previous studies showed that BLA use-dependently blocked Nav1.3, Nav1.7, and Nav1.8 in cell lines at a higher concentration ($10 \mu\text{M}$).^{21,22} In the present work, we investigated whether BLA at IC₅₀ concentrations of resting state in each channel subtype has the same effect. To do this, Na⁺ currents elicited by 100 pulses (from -80 mV to -10 mV) with different frequencies were recorded before and 15 min after BLA application. When stimulated with 1 Hz (100 pulses), BLA significantly reduced the currents of Nav1.7 and Nav1.8 but not of Nav1.3 (Figure 7(a) to (c)). When stimulation frequency increased to 3 or 10 Hz, the Na⁺ currents of Nav1.3 and Nav1.7 reduced further, while Nav1.8 currents did not do so (Figure 7(d) to (i)). As shown in Figure 7(j), the net inhibitory rate for Nav1.3 and Nav1.7 but not for Nav1.8 currents enhanced with increasing frequency and was highest for Nav1.7, less for Nav1.3.

BLA accelerates the inactivation of Nav1.3, Nav1.7, and Nav1.8 subtypes

The effects of the BLA on the activation, inactivation, and recovery of Nav1.3, Nav1.7, and Nav1.8 at corresponding IC₅₀ concentrations were also evaluated. The inactivation curves shifted significantly in the hyperpolarizing direction after BLA application (Figure 8(d) to (f) and Table 2), while activation curves (Figure 8(a)

to (c) and Table 2) and recovery curves (Figure 8(g) to (i) and Table 2) did not change in all channel subtypes.

Discussion

In the present work, we showed for the first time that BLA at 5 nM inhibited the hyperexcitability of DRG neurons in SNI rats. BLA preferably blocked TTX-S Nav channels over TTX-R ones and was more potent for blocking inactivated channels than resting channels in DRG neurons of SNI rats. BLA preferably blocked Nav1.3, Nav1.7 over Nav1.8, and the effect was more potent on inactivated than resting Nav channels in cell lines. The use-dependent blockage of BLA on Nav1.7 and Nav1.3 was also stronger than that on Nav1.8 at IC₅₀ concentrations. BLA accelerated the inactivation of Nav1.3, Nav1.7, and Nav1.8 subtypes but did not affect their activation and recovery at IC₅₀ concentrations. The preferable effects on inactivated TTX-S Nav1.3 and Nav1.7 may explain the clinical finding that oral BLA is effective for treatment of chronic pain.^{15,16}

BLA reduce the hyperexcitability of DRG neurons induced by SNI

Clinical studies show that oral administration of BLA is effective for relief of arthralgia and neck shoulder lumbocentral pain.^{15,16} The former belongs to inflammatory pain, while the latter is caused by intervertebral disc degeneration, in which both nociceptive pain and neuropathic pain are involved.³⁷ Recently, we showed that oral administration of BLA attenuates neuropathic pain induced by paclitaxel in rats¹⁹ and that local application of BLA (1 and 10 nM) onto L4-6 DRGs ipsilateral to surgery depressed the behavioral signs of neuropathic pain induced by L5 spinal nerve ligation.²⁰ In the present work, we further showed BLA at 5 nM reversed the decreased threshold of action potentials and

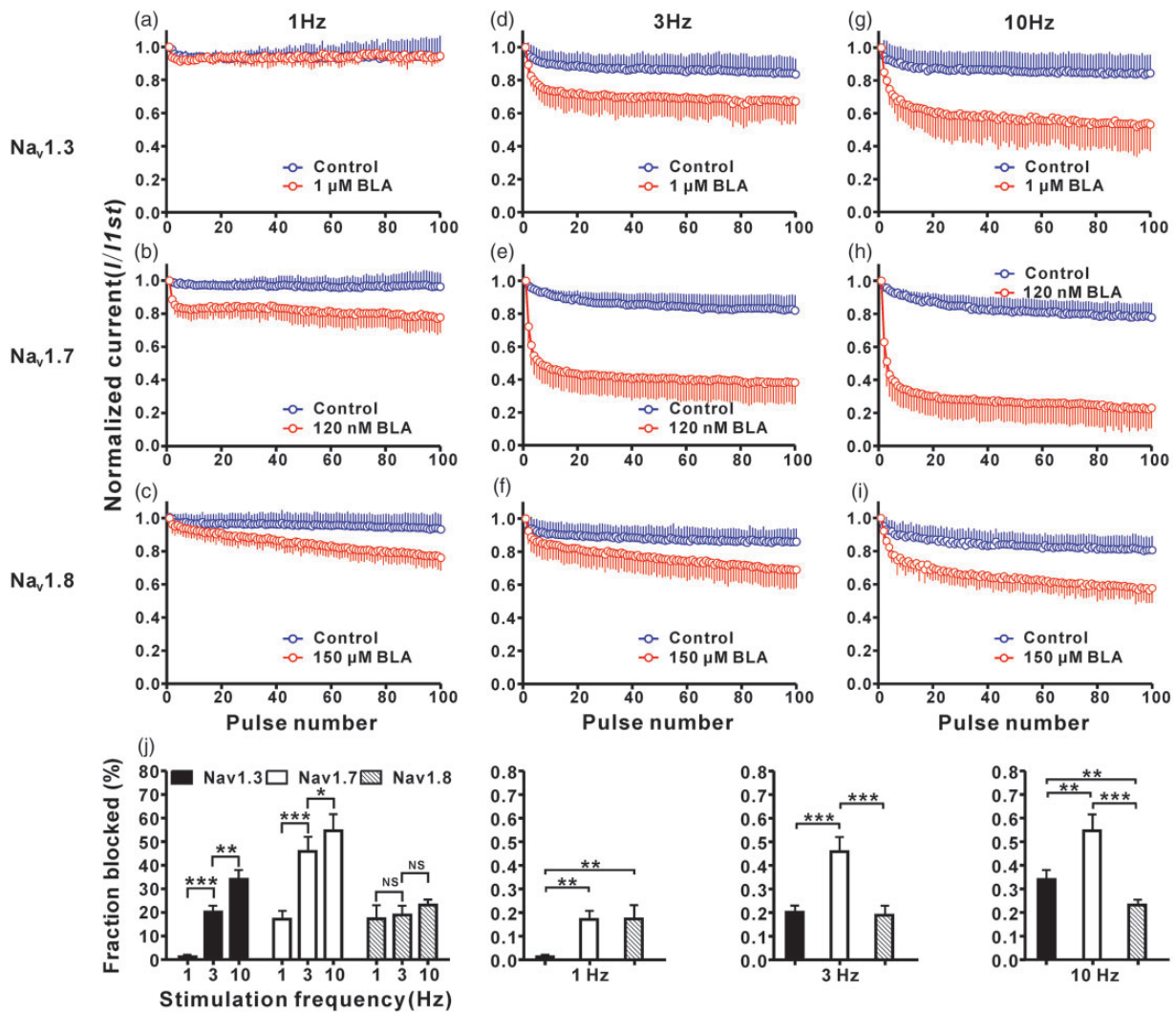


Figure 7. Use-dependent blockage of BLA on Nav1.3, Nav1.7, and Nav1.8 with different potencies. (a) to (i) The normalized amplitudes of Na⁺ currents evoked by 100 pulses in the absence (control) and presence of BLA at IC₅₀ concentrations. (j) The net inhibitory rates for Nav1.3, Nav1.7, and Nav1.8 currents in different frequencies are shown. **p* < 0.05, ***p* < 0.01, ****p* < 0.001. ns: not significant (*n* = 9 cells in each test).

the increased firing rate of DRG neurons isolated from SNI rats but not from sham rats but did not affect input resistance. BLA preferably blocked TTX-S Nav channels over TTX-R ones and was more potent for blocking inactivated channels than resting channels in DRG neurons of SNI rats. The effects of BLA are similar to those of carvacrol, another natural compound isolated from essential oils of plants, which reduces excitability and blocks Nav channel without affecting input resistance of DRG neurons.^{38,39}

Recently, it was reported that BLA inhibited neuropathic pain by stimulating dynorphin A expression in spinal microglia.⁴⁰ The result is inconsistent with previous works showing that spinal dynorphin A promotes but not inhibits neuropathic pain.⁴¹⁻⁴³

BLA preferably blocks TTX-S Nav1.3, Nav1.7 over TTX-R Nav1.8 and is more potent for blocking inactivated channels

As mentioned in introduction, TTX-S Nav1.3, Nav1.7, and TTX-R Nav1.8 are critically involved in neuropathic pain. The present work showed that in DRG neurons from ipsilateral side of injury, IC₅₀ for resting TTX-S Nav channels was 25 times lower than that for TTX-R Nav channels (3.8 ± 0.4 nM vs. 94.6 ± 11.5 nM). IC₅₀ values for inactivated TTX-S and TTX-R Nav channels (0.5 ± 0.1 nM and 8.0 ± 1.0 nM) were at least eight times lower compared to those for resting channels. Although BLA was less effective on Nav channels in DRG neurons from contralateral side of injury, it also preferably

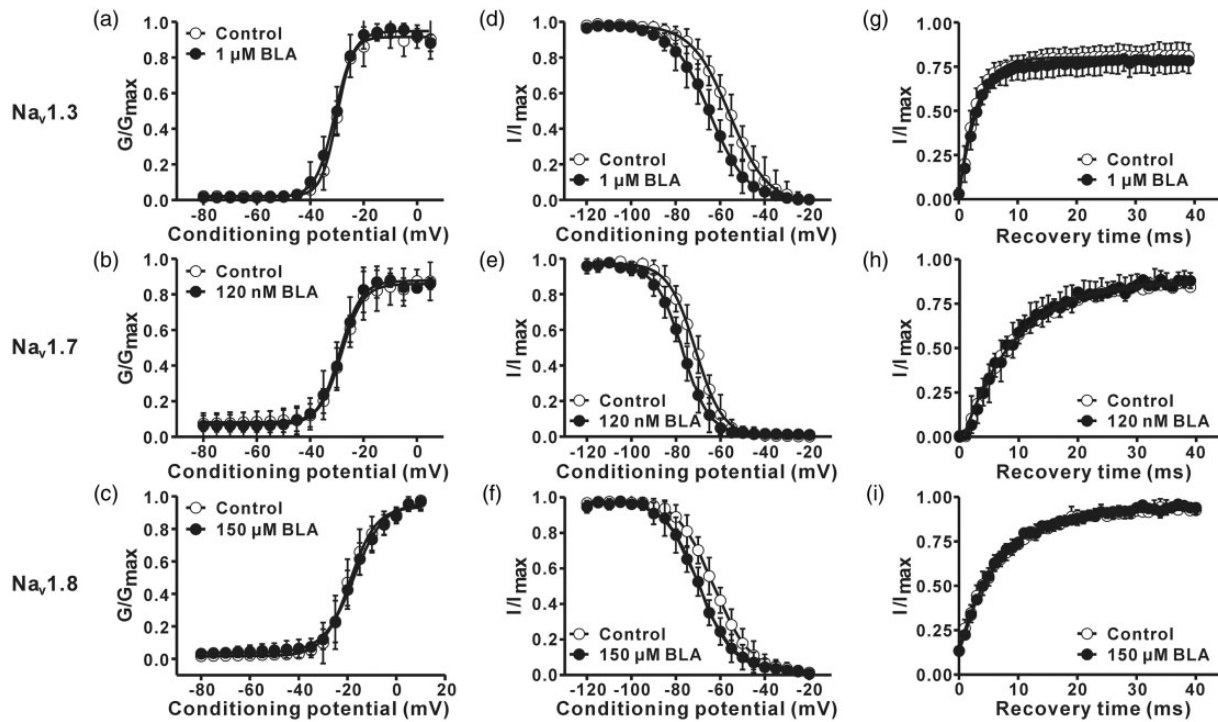


Figure 8. The effects of BLA on the activation, inactivation, and recovery of Nav1.3, Nav1.7, and Nav1.8 at corresponding IC₅₀ concentrations. (a) to (c) The activation curves show that BLA did not affect activation of Nav1.3, Nav1.7, and Nav1.8 ($p > 0.05$, $n = 10$ in each group). (d) to (f) The inactivation curves indicated that BLA speeded inactivation of Nav1.3, Nav1.7, and Nav1.8 ($p < 0.05$ vs. corresponding control, $n = 11$ in each group). (g) to (i) The recovery from inactivation of all channel subtypes was not affected by BLA ($p > 0.05$, $n = 8$ in each group). The detailed parameter analysis is shown in Table 2.

Table 2. Parameters for Nav channel subtypes activation, inactivation, and recovery in cell lines.

		Activation		Inactivation		Recovery	
		V _{0.5}	k	V _{0.5}	k	τ	
Nav1.3	Control	-30.01 ± 1.49	2.93 ± 0.37	-55.69 ± 2.08	8.56 ± 0.74	2.93 ± 0.37	
	BLA	-30.72 ± 1.36	3.61 ± 0.50	-64.58 ± 1.55**	8.35 ± 0.92	3.07 ± 0.20	
Nav1.7	Control	-28.19 ± 1.46	4.01 ± 1.01	-71.14 ± 1.24	6.16 ± 0.41	8.94 ± 0.79	
	BLA	-28.93 ± 1.49	4.08 ± 0.32	-77.15 ± 1.37*	6.03 ± 1.49	8.98 ± 0.71	
Nav1.8	Control	-19.01 ± 1.41	5.43 ± 0.36	-63.68 ± 2.11	7.63 ± 0.49	7.17 ± 0.51	
	BLA	-17.47 ± 1.74	6.10 ± 0.69	-69.37 ± 1.42*	6.23 ± 0.52	7.06 ± 0.54	

Note: Mean values were derived from Boltzmann equation fits of individual data sets as described in the measures.

BLA: Bulleyaconitine A.

* $p < 0.05$, ** $p < 0.01$ versus corresponding control, compared by two-tailed paired Student t test.

blocked TTX-S Nav channels over TTX-R Nav channels and was more potent for inactivated channels. Consistently, in cell lines BLA also more potent for blocking resting and inactivated Nav1.7 and Nav1.3 than Nav1.8. IC₅₀ for inactivated Nav1.3, Nav1.7, and Nav1.8 (20.3 ± 3.4 pM, 132.9 ± 25.5 pM, and 18.0 ± 2.5 μM) were much lower than those for resting channels (995.6 ± 139.1 nM, 125.7 ± 18.6 nM, and 151.2 ± 15.4 μM). The preferable effects on TTX-S and inactivated sodium channels are clinically interesting, because

previous studies on rats show the peak plasma concentration of BLA is 17.8 nM (11.4 ng/ml) following a single oral administration at 0.36 mg/kg²³ and that oral BLA at 0.4 mg/kg is effective for attenuation of the behavioral signs of neuropathic pain produced by paclitaxel in rats.¹⁹ Accordingly, therapeutic dose of oral BLA is only sufficient to block resting and inactivated TTX-S and inactivated TTX-R channels in DRG neurons, and inactivated Nav1.3 and Nav1.7 in cell lines. As both Nav1.3 and Nav1.7 subtypes are important for setting

the threshold and the firing rate of action potentials,^{44–47} it is not surprising to see that BLA diminished the hyperexcitability of DRG neurons in SNI rats at a concentration as low as 5 nM in vitro. The preferable blockage of BLA on inactivated Nav1.3 and Nav1.7 may also explain the BLA-induced enhancement of the half-widths of action potentials, reduction of the peak amplitude and overshoot, acceleration of the rising phase of action potentials. Taken together, oral administration of BLA may inhibit the hyperexcitability of DRG neurons by blocking TTX-S Nav channels, contributing to relief of neuropathic pain.

The important role of use-dependent block for antineuropathic pain

The use-dependent blockade of Nav channel is clinically important for treatment of arrhythmias and epilepsy because of selective blockage of the channels that opens with high frequency (see literature³⁴ for a review). In the case of neuropathic pain, the spontaneous activity in primary afferents ranges from 0.2 to 50 Hz in L5-SNL rats.⁴⁸ In the present work, we showed that BLA use-dependently blocked Nav1.3, Nav1.7 but not Nav1.8 at IC₅₀ concentrations. The strongest effect was observed on Nav1.7, less on Nav1.3. Apparently, the selective use-dependent blockage of Nav1.3 and Nav1.7 of BLA may contribute to its antineuropathic pain effect.

At present, the mechanisms underlying the use-dependent blockage of BLA on Nav1.3 and Nav1.7 are unclear. Upon activated, Na⁺ channels rapidly switches from the resting state to the open, inactivated state, and eventually back to resting state. Our previous literature²⁰ and present work show that BLA preferably inhibited inactivated sodium channels over resting ones, and this may contribute to the use-dependent effect by reduction of the numbers of resting channels during the repetitive activation. Further studies are needed to clarify the mechanisms underlying the preferable effect of BLA on inactivated Na⁺ channels.

It is well established that a loss of function of Nav1.7 in humans renders people unable to experience pain,⁴⁹ while gain-of-function missense mutations of the human Nav1.7 causes inherited primary erythralgia and paroxysmal extreme pain disorder.^{50,51} The present work revealed that BLA potently blocked resting, inactivated and opening Nav1.7. We, therefore, suggested that the drug may be effective for relief of the severe pain associated with Nav1.7 mutation. This should be tested clinically.

As alteration of other channels in DRG neurons, such as voltage-gated calcium channels and hyperpolarization-activated cyclic nucleotide-gated ion channels are also involved in the neuropathic pain,¹⁰ it

is possible that BLA may also target channels other than Nav channels. Further studies are needed to test the hypothesis.

In conclusion, BLA preferably blocked TTX-sensitive Nav1.3 and Nav1.7 over TTX-resistant Nav1.8 and is more potent for blocking inactivated channels. The use-dependent blockage of BLA was most profound on Nav1.7, less on Nav1.3, and least on Nav1.8 and facilitated the inactivation of Nav1.3, Nav1.7, and Nav1.8. BLA may inhibit neuropathic pain by inhibition of hyperexcitability of DRG neurons via blocking Nav channels.

Declaration of Conflicting Interests

The author(s) declared no potential conflicts of interest with respect to the research, authorship, and/or publication of this article.

Funding

The author(s) disclosed receipt of the following financial support for the research, authorship, and/or publication of this article: This work was supported by grants from the National Natural Science Foundation of China (U1201223, 31771166).

References

1. Finnerup NB, Attal N, Haroutounian S, McNicol E, Baron R, Dworkin RH, Gilron I, Haanpaa M, Hansson P, Jensen TS, Kamerman PR, Lund K, Moore A, Raja SN, Rice AS, Rowbotham M, Sena E, Siddall P, Smith BH and Wallace M. Pharmacotherapy for neuropathic pain in adults: a systematic review and meta-analysis. *Lancet Neurol* 2015; 14: 162–173.
2. Baron R, Binder A and Wasner G. Neuropathic pain: diagnosis, pathophysiological mechanisms, and treatment. *Lancet Neurol* 2010; 9: 807–819.
3. Serra J, Bostock H, Sola R, Aleu J, Garcia E, Cokic B, Navarro X and Quiles C. Microneurographic identification of spontaneous activity in C-nociceptors in neuropathic pain states in humans and rats. *Pain* 2012; 153: 42–55.
4. Stemkowski PL and Smith PA. Sensory neurons, ion channels, inflammation and the onset of neuropathic pain. *Can J Neurol Sci* 2012; 39: 416–435.
5. Shen KF, Zhu HQ, Wei XH, Wang J, Li YY, Pang RP and Liu XG. Interleukin-10 down-regulates voltage gated sodium channels in rat dorsal root ganglion neurons. *Exp Neurol* 2013; 247: 466–475.
6. Chen X, Pang RP, Shen KF, Zimmermann M, Xin WJ, Li YY and Liu XG. TNF-alpha enhances the currents of voltage gated sodium channels in uninjured dorsal root ganglion neurons following motor nerve injury. *Exp Neurol* 2011; 227: 279–286.
7. Djouhri L, Fang X, Koutsikou S and Lawson SN. Partial nerve injury induces electrophysiological changes in conducting (uninjured) nociceptive and nonnociceptive DRG neurons: possible relationships to aspects of

- peripheral neuropathic pain and paresthesias. *Pain* 2012; 153: 1824–1836.
8. Pexton T, Moeller-Bertram T, Schilling JM and Wallace MS. Targeting voltage-gated calcium channels for the treatment of neuropathic pain: a review of drug development. *Expert Opin Investig Drugs* 2011; 20: 1277–1284.
 9. Postea O and Biel M. Exploring HCN channels as novel drug targets. *Nat Rev Drug Discov* 2011; 10: 903–914.
 10. Tibbs GR, Posson DJ and Goldstein PA. Voltage-gated ion channels in the PNS: novel therapies for neuropathic pain? *Trends Pharmacol Sci* 2016; 37: 522–542.
 11. Samad OA, Tan AM, Cheng X, Foster E, Dib-Hajj SD and Waxman SG. Virus-mediated shRNA knockdown of Nav1.3 in rat dorsal root ganglion attenuates nerve injury-induced neuropathic pain. *Mol Ther* 2013; 21: 49–56.
 12. Sadamasu A, Sakuma Y, Suzuki M, Orita S, Yamauchi K, Inoue G, Aoki Y, Ishikawa T, Miyagi M, Kamoda H, Kubota G, Oikawa Y, Inage K, Sainoh T, Sato J, Nakamura J, Toyone T, Takahashi K and Ohtori S. Upregulation of Nav1.7 in dorsal root ganglia after intervertebral disc injury in rats. *Spine* 2014; 39: E421–E426.
 13. Joshi SK, Mikusa JP, Hernandez G, Baker S, Shieh CC, Neelands T, Zhang XF, Niforatos W, Kage K, Han P, Krafft D, Falztynek C, Sullivan JP, Jarvis MF and Honore P. Involvement of the TTX-resistant sodium channel Nav 1.8 in inflammatory and neuropathic, but not post-operative, pain states. *Pain* 2006; 123: 75–82.
 14. Waxman SG, Merkies IS, Gerrits MM, Dib-Hajj SD, Lauria G, Cox JJ, Wood JN, Woods CG, Drenth JP and Faber CG. Sodium channel genes in pain-related disorders: phenotype-genotype associations and recommendations for clinical use. *Lancet Neurol* 2014; 13: 1152–1160.
 15. Chen XY, Xia XL, Xiong JM and Tai PY. The analgesic anti-inflammatory effects of BLA tablets: clinical observation on 134 cases. *Yunnan J Tradit Chin Med Mater Med* 1996; 17: 54–55.
 16. Liu YQ, Ding XN and Wang YD. The clinical studies of BLA tablets to treat common chronic pain. *Chin J Pain Med* 2011; 17: 314–315.
 17. Tang XC. Bulleyaconitine A, a new analgesic and anti-inflammatory agent. *New Drug Clin* 1986; 5: 120–121.
 18. Weng WY, Xu HN, Li H, Shen T, Zhang JF, Shao L and Qian LH. Skin permeability and anti-inflammatory analgesic activities of Bulleyaconitine A liposomes. *Chin J Clin Pharm* 2003; 7: 131–135.
 19. Zhu HQ, Xu J, Shen KF, Pang RP, Wei XH and Liu XG. Bulleyaconitine A depresses neuropathic pain and potentiation at C-fiber synapses in spinal dorsal horn induced by paclitaxel in rats. *Exp Neurol* 2015; 273: 263–272.
 20. Xie MX, Pang RP, Yang J, Shen KF, Xu J, Zhong XX, Wang SK, Zhang XL, Liu YQ and Liu XG. Bulleyaconitine A preferably reduces tetrodotoxin-sensitive sodium current in uninjured dorsal root ganglion neurons of neuropathic rats probably via inhibition of protein kinase C. *Pain* 2017; 158: 2169–2180.
 21. Wang CF, Gerner P, Wang SY and Wang GK. Bulleyaconitine A isolated from aconitum plant displays long-acting local anesthetic properties in vitro and in vivo. *Anesthesiology* 2007; 107: 82–90.
 22. Wang CF, Gerner P, Schmidt B, Xu ZZ, Nau C, Wang SY, Ji RR and Wang GK. Use of Bulleyaconitine A as an adjuvant for prolonged cutaneous analgesia in the rat. *Anesth Analg* 2008; 107: 1397–1405.
 23. Xu HR, Ji GX, Wang Q, Li XN, Gong YJ, Zhang Y, Li W and Shen T. Dose-dependent pharmacokinetics of Bulleyaconitine A in rats. *Pharmazie* 2013; 68: 170–172.
 24. Zimmermann M. Ethical guidelines for investigations of experimental pain in conscious animals. *Pain* 1983; 16: 109–110.
 25. Decosterd I and Woolf CJ. Spared nerve injury: an animal model of persistent peripheral neuropathic pain. *Pain* 2000; 87: 149–158.
 26. Lyu YS, Park SK, Chung K and Chung JM. Low dose of tetrodotoxin reduces neuropathic pain behaviors in an animal model. *Brain Res* 2000; 871: 98–103.
 27. Wei XH, Zang Y, Wu CY, Xu JT, Xin WJ and Liu XG. Perisciatric administration of recombinant rat TNF-alpha induces mechanical allodynia via upregulation of TNF-alpha in dorsal root ganglia and in spinal dorsal horn: the role of NF-kappa B pathway. *Exp Neurol* 2007; 205: 471–484.
 28. Huang ZJ and Song XJ. Differing alterations of sodium currents in small dorsal root ganglion neurons after ganglion compression and peripheral nerve injury. *Mol Pain* 2008; 4: 20.
 29. Wang Y, Mi J, Lu K, Lu Y and Wang K. Comparison of gating properties and use-dependent block of Nav1.5 and Nav1.7 channels by anti-arrhythmics mexiletine and lidocaine. *PLoS One* 2015; 10: e0128653.
 30. Chahine M and O'Leary ME. Regulation/modulation of sensory neuron sodium channels. *Handb Exp Pharmacol* 2014; 221: 111–135.
 31. Tanaka K, Sekino S, Ikegami M, Ikeda H and Kamei J. Antihyperalgesic effects of ProTx-II, a Nav1.7 antagonist, and A803467, a Nav1.8 antagonist, in diabetic mice. *J Exp Pharmacol* 2015; 7: 11–16.
 32. Anreddy N, Zhang YK, Wang YJ, Shukla S, Kathawala RJ, Kumar P, Gupta P, Ambudkar SV, Wurlpel JN, Chen ZS and Guo H. A-803467, a tetrodotoxin-resistant sodium channel blocker, modulates ABCG2-mediated MDR in vitro and in vivo. *Oncotarget* 2015; 6: 39276–39291.
 33. Narahashi T and Roy ML. Differential properties of tetrodotoxin-sensitive and tetrodotoxin-resistant sodium channels in rat dorsal root ganglion neurons. *J Neurosci* 1992; 72: 2104–2111.
 34. Mantegazza M, Curia G, Biagini G, Ragsdale DS and Avoli M. Voltage-gated sodium channels as therapeutic targets in epilepsy and other neurological disorders. *Lancet Neurol* 2010; 9: 413–424.
 35. Fischer TZ, Gilmore ES, Estacion M, Eastman E, Taylor S, Melanson M, Dib-Hajj SD and Waxman SG. A novel Nav1.7 mutation producing carbamazepine-responsive erythromelalgia. *Ann Neurol* 2009; 65: 733–741.
 36. Lee JH, Park CK, Chen G, Han Q, Xie RG, Liu T, Ji RR and Lee SY. A monoclonal antibody that targets a Nav1.7 channel voltage sensor for pain and itch relief. *Cell* 2014; 157: 1393–1404.

37. Brisby H. Pathology and possible mechanisms of nervous system response to disc degeneration. *J Bone Joint Surg Am* 2006; 88: 68–71.
38. Joca HC, Cruz-Mendes Y, Oliveira-Abreu K, Maia-Joca RP, Barbosa R, Lemos TL, Lacerda Beirao PS and Leal-Cardoso JH. Carvacrol decreases neuronal excitability by inhibition of voltage-gated sodium channels. *J Nat Prod* 2012; 75: 1511–1517.
39. Joca HC, Vieira DC, Vasconcelos AP, Araujo DA and Cruz JS. Carvacrol modulates voltage-gated sodium channels kinetics in dorsal root ganglia. *Eur J Pharmacol* 2015; 756: 22–29.
40. Li TF, Fan H and Wang YX. Aconitum-derived Bulleyaconitine A exhibits antihypersensitivity through direct stimulating dynorphin A expression in spinal microglia. *J Pain* 2016; 17: 530–548.
41. Lai J, Luo MC, Chen Q, Ma S, Gardell LR, Ossipov MH and Porreca F. Dynorphin A activates bradykinin receptors to maintain neuropathic pain. *Nat Neurosci* 2006; 9: 1534–1540.
42. Vanderah TW, Gardell LR, Burgess SE, Ibrahim M, Dogrul A, Zhong CM, Zhang ET, Malan TP Jr, Ossipov MH, Lai J and Porreca F. Dynorphin promotes abnormal pain and spinal opioid antinociceptive tolerance. *J Neurosci* 2000; 20: 7074–7079.
43. Wang Z, Gardell LR, Ossipov MH, Vanderah TW, Brennan MB, Hochgeschwender U, Hruby VJ, Malan TP Jr, Lai J and Porreca F. Pronociceptive actions of dynorphin maintain chronic neuropathic pain. *J Neurosci* 2001; 21: 1779–1786.
44. Gold MS and Gebhart GF. Nociceptor sensitization in pain pathogenesis. *Nat Med* 2010; 16: 1248–1257.
45. Muroi Y, Ru F, Kollarik M, Canning BJ, Hughes SA, Walsh S, Sigg M, Carr MJ and Udem BJ. Selective silencing of Na(V)1.7 decreases excitability and conduction in vagal sensory neurons. *J Physiol* 2011; 589: 5663–5676.
46. Telinius N, Majgaard J, Kim S, Katballe N, Pahle E, Nielsen J, Hjortdal V, Aalkjaer C and Boedtkjer DB. Voltage-gated sodium channels contribute to action potentials and spontaneous contractility in isolated human lymphatic vessels. *J Physiol* 2015; 593: 3109–3122.
47. Cummins TR, Aglieco F, Renganathan M, Herzog RI, Dib-Hajj SD and Waxman SG. Nav1.3 sodium channels: rapid repriming and slow closed-state inactivation display quantitative differences after expression in a mammalian cell line and in spinal sensory neurons. *J Neurosci* 2001; 21: 5952–5961.
48. Liu X, Eschenfelder S, Blenk KH, Janig W and Habler H. Spontaneous activity of axotomized afferent neurons after L5 spinal nerve injury in rats. *Pain* 2000; 84: 309–318.
49. Cox JJ, Reimann F, Nicholas AK, Thornton G, Roberts E, Springell K, Karbani G, Jafri H, Mannan J, Raashid Y, Al-Gazali L, Hamamy H, Valente EM, Gorman S, Williams R, McHale DP, Wood JN, Gribble FM and Woods CG. An SCN9A channelopathy causes congenital inability to experience pain. *Nature* 2006; 444: 894–898.
50. Drenth JP and Waxman SG. Mutations in sodium-channel gene SCN9A cause a spectrum of human genetic pain disorders. *J Clin Invest* 2007; 117: 3603–3609.
51. Fertleman CR, Baker MD, Parker KA, Moffatt S, Elmslie FV, Abrahamsen B, Ostman J, Klugbauer N, Wood JN, Gardiner RM and Rees M. SCN9A mutations in paroxysmal extreme pain disorder: allelic variants underlie distinct channel defects and phenotypes. *Neuron* 2006; 52: 767–774.